

Submicrometer axial resolution optical coherence tomography

B. Povazay, K. Bizheva, A. Unterhuber, B. Hermann, H. Sattmann, A. F. Fercher, and W. Drexler

Institute of Medical Physics, Christian Doppler Laboratory, University of Vienna, Vienna A-1090, Austria

A. Apolonski

Photonics Institute, Christian Doppler Laboratory, Vienna University of Technology, Vienna, Austria

W. J. Wadsworth, J. C. Knight, and P. St. J. Russell

Optoelectronics Group, Department of Physics, University of Bath, Bath, UK

M. Vetterlein and E. Scherzer

Institute of Histology and Embryology, University of Vienna, Vienna, Austria

Received June 10, 2002

Optical coherence tomography (OCT) with unprecedented submicrometer axial resolution achieved by use of a photonic crystal fiber in combination with a compact sub-10-fs Ti:sapphire laser (Femtolasers Produktions) is demonstrated for what the authors believe is the first time. The emission spectrum ranges from 550 to 950 nm ($\lambda_c = 725$ nm, $P_{\text{out}} = 27$ mW), resulting in a free-space axial OCT resolution of ~ 0.75 μm , corresponding to ~ 0.5 μm in biological tissue. Submicrometer-resolution OCT is demonstrated *in vitro* on human colorectal adenocarcinoma cells HT-29. This novel light source has great potential for development of spectroscopic OCT because its spectrum covers the absorption bands of several biological chromophores. © 2002 Optical Society of America

OCIS codes: 110.4500, 170.3880, 060.7140, 190.4370.

Optical coherence tomography (OCT) is a non-invasive optical imaging technique that permits three-dimensional cross-sectional visualization of microstructural morphology in superficial regions of transparent and nontransparent biological tissue.^{1–3} Because OCT uses partially coherent light, the axial resolution of the image is determined by the temporal coherence of the light source. In the case of superluminescent diodes, the axial OCT resolution is typically limited to 10–15 μm ; for it to be enhanced, broad-bandwidth light sources are required. The first sub-10- μm -resolution OCT was achieved by use of the broadband fluorescence from Ti:sapphire.⁴ Biological imaging could not be performed with this type of light source because of its low brightness. Despite their broad emission bandwidths, current incandescent light sources provide insufficient intensity in a single spatial mode that is necessary for high-speed raster imaging in nontransparent biological tissue.^{5,6} Recently a state-of-the-art broadband Ti:sapphire laser was developed for 1- μm axial-resolution spectroscopic OCT imaging.^{7–9} Lately it was demonstrated that photonic crystal fibers¹⁰ (PCFs) or tapered fibers¹¹ can be used to generate an extremely broadband continuum by use of low-energy femtosecond pulses. Because of the limited gain bandwidth of the Ti:sapphire crystal, such a spectral bandwidth can never be generated directly by a Ti:sapphire laser. As was recently demonstrated, utilization of a PCF-based light source in OCT systems results in ~ 2 - μm axial resolution for emission spectra located near 1300 nm.¹²

In this Letter we demonstrate what is to our knowledge the first submicrometer-resolution OCT achieved by use of a PCF pumped with a compact, commercially available sub-10-fs Ti:sapphire laser. A stable, slightly modulated spectrum ranging from 550 to 950 nm (at its pedestal) with an output power of a

few tens of milliwatts was generated with this source, thus facilitating in-depth imaging of biological tissue with unprecedented axial resolution.

Until recently, PCFs were used only in combination with conventional 100-fs Ti:sapphire oscillators.^{10,12} In a previous study, multiple approaches to generating a smooth, powerful, and stable supercontinuum in a cobweb PCF were undertaken with sub-20-fs pulses with various chirp, power, and polarization states as well as fibers of various lengths and core sizes.¹³ According to that study, short (a few millimeters in length) fibers in combination with sub-20-fs pulses tend to generate broad spectra with minimal modulation, expanded mainly toward the visible wavelength range. Hence in the present study a 2.3- μm core diameter, 6-mm length PCF (University of Bath, UK) was pumped with a compact, commercially available Ti:sapphire laser (Femtsource Compact Pro, Femtolasers Produktions) emitting sub-10-fs pulses with an ~ 100 -MHz repetition rate and an output power of as much as 400 mW to generate a relatively smooth supercontinuum, spanning a FWHM of more than 325 nm. The fiber was cut at an angle to prevent backreflection to the oscillator. The oscillator pulses were prechirped by undergoing 20 bounces on chirped mirrors. Quarter- and half-wave plates were used to select a particular polarization state of the incident beam and thus to shape the emitted spectrum.¹³ A set of achromatic doublet lenses (Fig. 1, L1 and L2) designed for optimal performance in the range 600–1000 nm, with N.A. of 0.6 and 0.3, respectively, were used to couple the incident beam into the PCF and to collimate the broadband output that was generated.

The supercontinuum generated by the PCF-based source was interfaced to a free-space OCT system (Fig. 1). A broadband achromatic lens (L3;

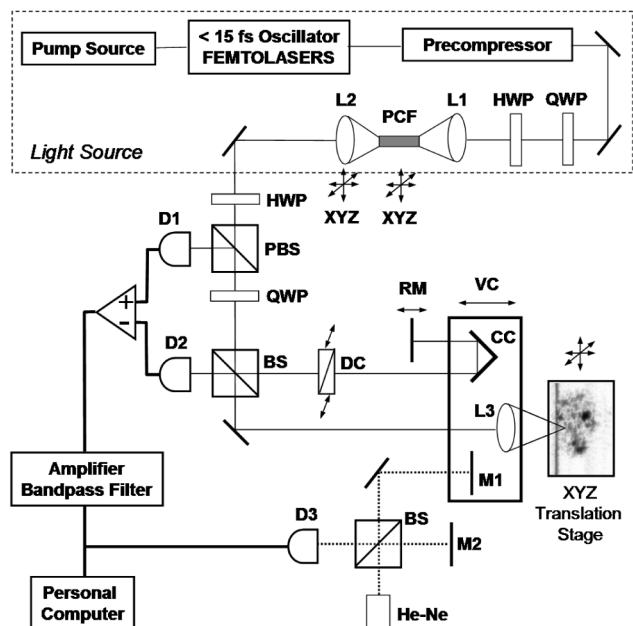


Fig. 1. Submicrometer-resolution OCT system: BSs, beamsplitters; PBS, polarization beam splitter; QWPs and HWPs, quarter-wave and half-wave plates, respectively; VC, voice coil; CC, corner cube; L's, lenses; D1–D3, detectors; DC, dispersion compensation; M1, M2, mirrors; RM, reference mirror; PCF, photonic crystal fiber.

$f = 10$ mm; N.A., 0.25) was used to focus the light onto the sample. Dynamic focusing was implemented to counteract the out-of-focus image degradation. Interferometric triggering was used to account for nonlinearities in the scanning rate of the voice coil scanner. Dual balanced detection was utilized to cancel the excess noise generated by the light source. An optical circulator that comprised a polarized beam splitter and quarter- and half-wave plates was used to optimize the power throughput of the system and to improve its sensitivity. All optical components of the OCT system were selected to provide optimal performance in the 400–1000-nm wavelength range. Dispersion compensation was achieved with a pair of BK7 prisms. The full interference fringe signal was digitized with a 10-Msamples/s, 16-bit resolution analog-to-digital converter followed by software demodulation. Consequently, a single measurement with the same instrument permits submicrometer axial resolution OCT imaging as well as extraction of spatially resolved spectroscopic information.⁹

Figure 2 shows the emission spectra [Fig. 2(a)] and the corresponding interference signal [Fig. 2(b)] produced by coupling of the PCF-based light source to the free-space interferometer. By proper selection of the input pulse parameters and PCF characteristics, a spectrum spanning 325 nm (at FWHM), centered at 725 nm, with spectral modulations less than 1.5 dB and a power output of as much as 27 mW was generated. By interfacing the PCF source with the interferometer and using a standard resolution chart we measured free-space OCT resolution of $2.5 \mu\text{m}$ in the lateral and $0.75 \mu\text{m}$ in the axial direction (corresponding to $0.5 \mu\text{m}$ in bio-

logical tissue). The axial resolution was defined as the FWHM of the envelope of the measured interferogram. Recently a similar OCT interference pattern was achieved with a thermal light source, although in that case the corresponding free-space axial resolution was $1.2 \mu\text{m}$ owing to the longer central wavelength (840 nm) and the smaller bandwidth (260 nm).⁶ The sensitivity of our system was evaluated to be 87 dB in free space for 1 mW of power at the sample surface. Sidelobes observed in the interferogram, caused by modulations in the light source's emission spectrum, were less than 5% of the signal maximum.

To demonstrate OCT in tissue with submicrometer axial resolution we imaged human colorectal adenocarcinoma cells HT-29 *in vitro*. Monolayers of cultured cells were grown upon coverslips at 37°C in a humidified atmosphere of 95% air and 5% CO_2 . The OCT images were acquired 48 h after seeding. Subsequently the cells were fixed and stained, and histological sections of $1\text{-}\mu\text{m}$ thickness in directions parallel and perpendicular to the OCT imaging direction were prepared. Multiple OCT cross-sectional images of a group of HT-29 cells were acquired *in vitro* with $0.5\text{-}\mu\text{m}$ axial and $\sim 2\text{-}\mu\text{m}$ transverse resolution, at 91-mm/s scanning speed

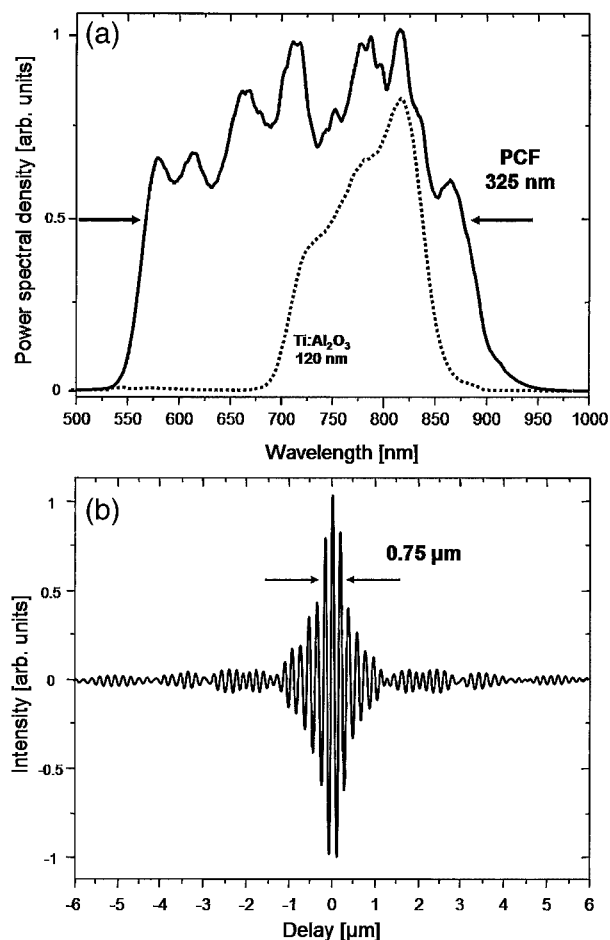


Fig. 2. (a) Optical spectrum of PCF output (solid curve), PCF input spectrum (dashed curve), and (b) corresponding interference signal.

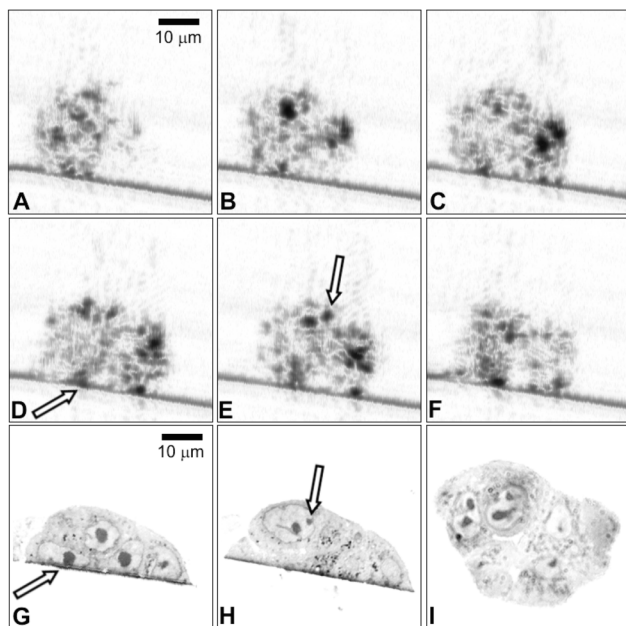


Fig. 3. *In vitro* submicrometer-resolution OCT images of human colorectal adenocarcinoma cells HT-29 with $0.5\text{-}\mu\text{m}$ axial and $\sim 2\text{-}\mu\text{m}$ transverse resolution, covering an area of $50\ \mu\text{m} \times 50\ \mu\text{m}$, equally spaced by $2\ \mu\text{m}$ (A–F). Arrows indicate features that may correspond to nucleoli of approximately $3\text{--}5\ \mu\text{m}$ diameter. Histological sections parallel (G and H) and perpendicular (I) to the OCT imaging direction of typical HT-29 cells.

and a 10-Hz scanning rate, covering an area of $50\ \mu\text{m} \times 50\ \mu\text{m}$ (500×500 pixels) and equally spaced by $2\ \mu\text{m}$ (Figs. 3A–3F). The image postprocessing procedure involved low-pass filtering, smoothing, and optimization of the image contrast. Histological sections of typical HT-29 cells parallel (Figs. 3G and 3H) and perpendicular (Fig. 3I) to the OCT imaging direction are displayed for better interpretation of the OCT tomograms. Comparison with histology demonstrates that submicrometer-resolution OCT images reveal features that may correspond to subcellular structures such as nucleoli (indicated by arrows in the figure) with approximately $2\text{--}3\text{-}\mu\text{m}$ diameter as well as to aggregates of cellular organelles.

In conclusion, using a compact, commercially available sub-10-fs Ti:sapphire laser, we have developed a PCF-based light source and used it to facilitate unprecedented submicrometer axial OCT resolution. This light source represents an improvement by a factor of 2 compared with previously used sources⁷ and, for the first time to our knowledge, permits the *in vitro* visualization of human subcellular structures

such as nucleoli. The broad bandwidth of the light source also provides access to a spectral region covering the absorption bands of a number of biological chromophores; thus this source has great potential for spectroscopic OCT.⁹

We gratefully acknowledge contributions by L. Schachinger, University of Vienna; M. Pavelka, J. Neumüller, and N. Niapir, Institute of Histology, University of Vienna; A. Stingl, A. Poppe, and G. Jung, Femtolasers; and F. Krausz and G. Tempea, Photonics Institute, Vienna University of Technology. This research was supported in part by grants FWF P14218-PSY and FWF Y 159-PAT from Fonds zur Förderung Wissenschaftlicher Forschung and CRAF-1999-70549 from the European Community, and by the Christian Doppler Society and Femtolasers Produktions. W. Drexler's e-mail address is wolfgang.drexler@univie.ac.at.

References

1. D. Huang, E. A. Swanson, C. P. Lin, J. S. Schuman, W. G. Stinson, W. Chang, M. R. Hee, T. Flotte, K. Gregory, C. A. Puliafito, and J. G. Fujimoto, *Science* **254**, 1178 (1991).
2. J. G. Fujimoto, M. E. Brezinski, G. J. Tearney, S. A. Boppart, B. Bouma, M. R. Hee, J. F. Southern, and E. A. Swanson, *Nature Med.* **1**, 970 (1995).
3. A. F. Fercher, *J. Biomed. Opt.* **1**, 157 (1996).
4. X. Clivaz, F. Marquis-Weible, and R. P. Salathé, *Electron. Lett.* **28**, 1553 (1994).
5. A. F. Fercher, C. K. Hitzenberger, M. Sticker, E. Morena-Barriuso, R. Leitgeb, W. Drexler, and H. Sattmann, *Opt. Commun.* **185**, 57 (2000).
6. L. Vabre, A. Dubois, and C. Boccara, *Opt. Lett.* **27**, 530 (2002).
7. W. Drexler, U. Morgner, F. X. Kärtner, C. Pitris, S. A. Boppart, X. D. Li, E. P. Ippen, and J. G. Fujimoto, *Opt. Lett.* **24**, 1221 (1999).
8. W. Drexler, U. Morgner, R. K. Ghanta, J. S. Schuman, F. Kärtner, and J. G. Fujimoto, *Nature Med.* **7**, 502 (2001).
9. U. Morgner, W. Drexler, F. X. Kärtner, X. D. Li, C. Pitris, E. P. Ippen, and J. G. Fujimoto, *Opt. Lett.* **25**, 111 (2000).
10. J. K. Ranka, R. S. Windeler, and A. J. Stentz, *Opt. Lett.* **25**, 25 (2000).
11. T. A. Birks, W. J. Wadsworth, and P. St. J. Russell, *Opt. Lett.* **25**, 1415 (2000).
12. I. Hartl, X. D. Li, C. Chudoba, R. K. Ghanta, T. K. Ko, J. G. Fujimoto, J. K. Ranka, and P. S. Windeler, *Opt. Lett.* **26**, 608 (2001).
13. A. Apolonski, B. Povazay, A. Unterhuber, T. A. Birks, W. J. Wadsworth, P. St. J. Russell, and W. Drexler, *J. Opt. Soc. Am. B* **19**, 2165 (2002).